Cellular/Molecular

Zones of Enhanced Glutamate Release from Climbing Fibers in the Mammalian Cerebellum

Martin Paukert,[1] Yanhua H. Huang,[1] Kohichi Tanaka,[3] Jeffrey D. Rothstein,[1,2] and Dwight E. Bergles[1]

[1]The Solomon H. Snyder Department of Neuroscience and [2]Department of Neurology, Johns Hopkins University School of Medicine, Baltimore, Maryland 21205, and [3]School of Biomedical Science and Medical Research Institute, Tokyo Medical and Dental University, Bunkyo-Ku, Tokyo 113-8510, Japan

Purkinje cells in the mammalian cerebellum are remarkably homogeneous in shape and orientation, yet they exhibit regional differences in gene expression. Purkinje cells that express high levels of zebrin II (aldolase C) and the glutamate transporter EAAT4 cluster in parasagittal zones that receive input from distinct groups of climbing fibers (CFs); however, the physiological properties of CFs that target these molecularly distinct Purkinje cells have not been determined. Here we report that CFs that innervate Purkinje cells in zebrin II-immunoreactive (Z^+) zones release more glutamate per action potential than CFs in Z^- zones. CF terminals in Z^+ zones had larger pools of release-ready vesicles, exhibited enhanced multivesicular release, and produced larger synaptic glutamate transients. As a result, CF-mediated EPSCs in Purkinje cells decayed more slowly in Z^+ zones, which triggered longer-duration complex spikes containing a greater number of spikelets. The differences in the duration of CF EPSCs between Z^+ and Z^- zones persisted in EAAT4 knock-out mice, indicating that EAAT4 is not required for maintaining this aspect of CF function. These results indicate that the organization of the cerebellum into discrete longitudinal zones is defined not only by molecular phenotype of Purkinje cells within zones, but also by the physiological properties of CFs that project to these distinct regions. The enhanced release of glutamate from CFs in Z^+ zones may alter the threshold for synaptic plasticity and prolong inhibition of cerebellar output neurons in deep cerebellar nuclei.

Introduction

Purkinje cells in the mammalian cerebellum receive powerful excitatory input from the inferior olive (IO) via climbing fibers (CFs), which convey information about the timing of motor commands (Kitazawa et al., 1998) and facilitate forms of synaptic plasticity that may underlie motor learning (Ito and Kano, 1982; Wang et al., 2000; Coesmans et al., 2004; Brenowitz and Regehr, 2005). Although the cellular organization of the cerebellar cortex is remarkably homogeneous, CFs arising from different regions of the IO segregate to form synapses with Purkinje cells in distinct longitudinal (rostrocaudal) zones (Sugihara at al., 2001). These CF inputs initiate synchronous firing of Purkinje cells within zones (Sasaki et al., 1989; Lang et al., 1999; Blenkinsop and Lang, 2006), because of the extensive electrical coupling among IO neurons, suggesting that compartmentalization of olivo-cerebellar signaling is fundamental to cerebellar function (Ozden et al., 2009).

Purkinje cells within these zones exhibit similar patterns of gene expression and can be identified based on the level of expression of the glycolytic enzyme aldolase C (zebrin II) (Brochu et al., 1990). Zones of zebrin II-immunoreactive (Z^+) Purkinje cells are symmetrically distributed, highly reproducible between individuals, and conserved across species (Hawkes and Gravel, 1991), yet the functional significance of these molecular differences are not well understood. Purkinje cells within Z^+ zones also express elevated levels of EAAT4 (Dehnes et al., 1998), a high-affinity transporter that removes glutamate at CF and parallel fiber synapses (Otis et al., 1997; Takayasu et al., 2005), and inhibitory input to Z^+ zones is enhanced (Gao et al., 2006), raising the possibility that Purkinje cells in these zones experience greater excitatory synaptic activity. Nevertheless, physiological differences between the CFs that target these distinct populations of Purkinje cells have not been described.

To evaluate whether the variations in gene expression exhibited by Purkinje cells reflect physiological differences between CF inputs, we compared the properties of CF–Purkinje cell synapses in Z^+ and Z^- zones within individual folia using *EAAT4-EGFP* mice (Gincel et al., 2007), in which Z^+ Purkinje cells can be visualized in living tissue. Our studies indicate that CFs within Z^+ zones release more glutamate per action potential, which slows the decay of CF EPSCs and induces longer-lasting complex spikes in Z^+ Purkinje cells. These physiological differences in CF signaling between cerebellar compartments may induce regional differences in the activity of output neurons in the deep cerebellar nuclei (DCN), because of the restricted targeting of Purkinje cell axons within the DCN (Sugihara et al., 2009), and alter the extent or duration of plasticity at CF and parallel fiber synapses. The increased expression of glycolytic enzymes and glutamate transporters by Purkinje cells in

Received Oct. 13, 2009; revised March 23, 2010; accepted April 5, 2010.

This work was supported by grants from the National Institutes of Health (NS44261 and NS50274) and the Center for Signaling to and from the Synapse (MH084020). We thank N. Nishiyama and N. Ye for help with animal breeding and genotyping; Richard Hawkes and Niels C. Danbolt for zebrin II and EAAT4 antibodies, respectively; Graham C. Ellis-Davies for MNI-D-aspartate; and members of the Bergles laboratory for helpful discussions.

Correspondence should be addressed to Dwight E. Bergles, The Solomon H. Snyder Department of Neuroscience, Johns Hopkins University School of Medicine, 725 North Wolfe Street, WBSB 1001, Baltimore, MD 21205. E-mail: dbergles@jhmi.edu.

Y.H. Huang's present address: Department of Veterinary and Comparative Anatomy, Pharmacology, and Physiology, Program in Neuroscience, Washington State University, 205 Wegner Hall, P.O. Box 646520, Pullman, WA 99164-6520.

DOI:10.1523/JNEUROSCI.5118-09.2010

 0270-6474/10/307290-10$15.00/0

Z^+ zones may help compensate for enhanced CF signaling in these regions.

Materials and Methods

Animals. *EAAT4-EGFP* mice were generated using the bacterial artificial chromosome (BAC) approach as described previously (Gincel et al., 2007). *EAAT4-EGFP* $^{+/+}$ mice were mated with C57BL/6 wild-type mice, and the progeny were used for all experiments.

Immunostaining. Mice [postnatal day 21 (P21) (see Fig. 1); P23 (see Fig. 7)] were perfused by cardiac puncture with 4% paraformaldehyde in phosphate buffer (PB) containing 80 mM Na_2HPO_4 and 20 mM KH_2PO_4, in accordance with animal welfare protocols approved by Johns Hopkins University. Brains were then removed and immersed in the same fixative for 4 h at 4°C. Free-floating coronal cerebellar sections [35 μm (see Fig. 1); 50 μm (see Fig. 7)] were prepared using a Vibratome (VT1000S; Leica) and collected in PB. Sections were rinsed, blocked against nonspecific antibody binding, and permeabilized in PB containing 5% normal donkey serum (NDS) and 1% Triton X-100 for 3 h. Sections were then incubated for 36 h at 4°C in PB containing 5% NDS, 0.5% Triton X-100, primary antibodies, rabbit α-EAAT4 (1:2000) and mouse α-zebrin II (1:200) (see Fig. 1), and guinea pig α-vGluT2 (1:6000; Millipore) (see Fig. 7). After rinsing, sections were incubated for 3 h at room temperature in PB containing 5% NDS and Cy3- and Cy5-conjugated secondary antibodies against rabbit and mouse IgG (1:400; Jackson ImmunoResearch) (see Fig. 1) and Cy5-conjugated secondary antibodies against guinea pig IgG (1:300; Jackson ImmunoResearch) (see Fig. 7). Images were obtained using a Nikon Eclipse E800 microscope equipped with a Retiga EX camera (QImaging) (see Fig. 1) and an AX10 Imager.M1 microscope equipped with an AxioCam HRm camera (both from Zeiss) (see Fig. 7). Images in Figure 1*A–F* are composites of six to eight separate images obtained using a 4× objective that were merged using Photoshop (Adobe Systems). White dotted lines show borders between each image. Images in Figure 1*G–I* were obtained using a 20× objective, and images in Figure 7 were obtained using a 5× objective. For the analysis of vGluT2 expression (see Fig. 7), regions of interest in Z^+ and Z^- zones were defined based on the intensity of enhanced green fluorescent protein (EGFP) fluorescence within $P1^+$ and $P2^+$ bands, or within $P1^-$ bands, in lobule VIII. For each section, the fraction of Z^- pixels that exceeded threshold (set at 95% of the pixel intensities measured within Z^+ zones) was determined using custom scripts written in Matlab (Mathworks).

Acute slice preparation. Cerebellar slices were prepared in the coronal orientation from 15- to 21-d-old mice (250 μm) on a vibratome in ice-cold cutting solution containing (in mM) 135 *N*-methyl-D-glucamine, pH adjusted to 7.4 with HCl, 1 KCl, 1.2 KH_2PO_4, 0.5 $CaCl_2$, 1.5 $MgCl_2$, 20 choline-HCO_3, and 11 glucose, saturated with 95% O_2/5% CO_2. Slices were incubated in artificial CSF (ACSF) containing (in mM) 119 NaCl, 2.5 KCl, 2.5 $CaCl_2$, 1.3 $MgCl_2$, 1 NaH_2PO_4, 26.2 $NaHCO_3$, and 11 glucose, saturated with 95% O_2/5% CO_2 at 37°C for 30 min and then allowed to recover for at least 30 min at room temperature before experimentation.

Electrophysiology. During recording, slices were constantly superfused with ACSF containing 5 μM 6-imino-3-(4-methoxyphenyl)-1(6*H*)-pyridazinebutanoic acid dihydrobromide (SR-95531) to block $GABA_A$ receptors. Slices were first examined at low power using a 4× objective and a CCD camera (XC-E130; Sony) to identify parasagittal bands near the vermis, denoted $P1^+$ to $P3^+$ from the midline moving laterally. Z^+ Purkinje cells within $P1^+$ and $P2^+$ bands, or Z^- Purkinje cells in $P1^-$ bands in lobule VIII, were selected based on the intensity of EGFP fluorescence (supplemental Fig. S1, available at www.jneurosci.org as supplemental material). Individual Purkinje cells were visualized through a 40× water-immersion objective using infrared light, differential interference contrast optics, and a CCD camera (XC-73; Sony). Recording electrodes were pulled from capillary tubing (#0010 glass; Corning) and had a combined resistance of 1.2–2.0 MΩ when filled with the internal solution. For whole-cell recordings, the pipette solution contained (in mM) 105 CsA (A represents NO_3^- or $CH_3O_3S^-$), 20 TEA-Cl, 10 Cs-EGTA, 20 HEPES, 1 $MgCl_2$, 2 Na_2-ATP, 0.2 Na-GTP, and 1 QX-314, pH adjusted to 7.3 for voltage-clamp recordings. All transporter currents were recorded with NO_3^- as the primary anion in the pipette solution. For current-clamp recordings, the pipette solution contained (in mM) 135 KCl, 20 HEPES, 1 $MgCl_2$, 2 Na_2-ATP, and 0.2 Na-GTP, pH adjusted to 7.3. The holding potential for voltage-clamp recordings was −70 mV for transporter currents and −15 mV for CF EPSCs. Synaptic transporter currents were recorded in the presence of 25 μM 2,3-dioxo-6-nitro-1,2,3,4-tetrahydrobenzo[*f*]quinoxaline-7-sulfonamide disodium salt (NBQX; an AMPA receptor antagonist). Access resistance was <10 MΩ, and experiments in which the access changed by >15% were not included for analysis. CFs were stimulated at 0.05 Hz with a patch pipette filled with ACSF, using a constant-current isolated stimulator (DS3; Digitimer) to supply a 50 μs pulse of 2–30 μA. The pipette position was adjusted to minimize the stimulus intensity required to generate an all-or-none CF-evoked response. Synaptic currents were recorded with a MultiClamp 700B amplifier (Molecular Devices), filtered at 2–3 kHz, and digitized at 10–50 kHz with a Digidata 1322A analog-to-digital converter (Molecular Devices). Complex spike recordings were filtered at 5 kHz and digitized at 50 kHz. To compare the effect of γ-D glutamylglycine (γ-DGG; a low-affinity AMPA receptor antagonist) on the CF paired-pulse ratio (PPR) between Purkinje cells from Z^+ and Z^- zones, we used ACSF containing 0.5 mM $CaCl_2$ and 3.3 mM $MgCl_2$, a condition that should reduce multivesicular release and increase the ability to detect differences in multivesicular release between CF synapses in Z^+ and Z^- zones. All recordings were made at room temperature.

Photolysis. Purkinje cells were locally superfused with HEPES-buffered saline containing (in mM) 137 NaCl, 2.5 KCl, 2.5 $CaCl_2$, 1.3 $MgCl_2$, and 20 HEPES, pH adjusted to 7.3. This solution contained 1 μM tetrodotoxin (a Na^+ channel blocker), 10 μM NBQX, 10 μM (*RS*)-3-(2-carboxypiperazin-4-yl)propyl-1-phosphonic acid (an NMDA receptor antagonist), 50 μM MK-801 [(5*R*,10*S*)-(+)-5-methyl-10,11-dihydro-5*H*-dibenzo[*a*,*d*]cyclohepten-5,10-imine hydrogen maleate; an NMDA receptor antagonist], 5 μM SR-95531, and 500 μM 4-carboxymethoxy-7-nitroindolinyl-D-aspartate (MNI-D-aspartate). The MNI-D-aspartate solution was applied using a wide-bore pipette (tip diameter, ~50 μm) fed by a 5 ml reservoir. Photolysis was induced by brief exposure (1 ms) to the UV output of an argon–ion laser (Stabilite 2017-AR; Spectra-Physics), as described previously (Huang et al., 2005). The output of the laser was focused to an ~100 μm spot using a 20× water-immersion objective (UMPlanFl; Olympus) that was centered on the dendritic arbor of the Purkinje cell. To control the length of exposure, a computer-controlled, programmable pulse generator (Master-8; AMP Instruments) was used to trigger a high-speed laser shutter placed between the laser head and the fiber launch. Miniature EPSCs (mEPSCs) were evoked by CF stimulation at 0.2 Hz at a holding potential of −70 mV with 1 mM $SrCl_2$ substituted for $CaCl_2$ and 2.8 or 4.0 mM $MgCl_2$. As there was no significant difference between events recorded in 2.8 or 4.0 mM $MgCl_2$, these data were pooled.

Data analysis. Data were analyzed off-line using pClamp (Molecular Devices) and Origin (OriginLab) software. For analysis of CF responses, traces obtained from subthreshold stimulation were averaged and subtracted from the response. Residual artifacts have been blanked for clarity in the figures. Illustrated traces represent two to five consecutive responses, except under low release probability conditions (see Fig. 5), in which 15 consecutive responses were averaged. Weighted decay was determined by measuring the integral of the normalized current trace from the peak to the time at which the response returned to baseline (Takayasu et al., 2005). mEPSCs were analyzed using the Mini Analysis Program (Synaptosoft) and were restricted to events that occurred within 1 s after CF stimulation, which had a maximal rise time of 1 ms, a tau decay of between 1 and 40 ms, and an amplitude of at least −20 pA. The last criterion was necessary, as substitution of $SrCl_2$ for $CaCl_2$ markedly increased membrane noise in mouse Purkinje cells, as reported previously (Maejima et al., 2001). Approximately 95% of events had a tau decay faster than 15 ms. Measurements of mEPSC amplitude or tau decay were obtained from recordings in which at least 150 or 50 events could be identified, respectively.

For variance–mean analysis, CF EPSCs were recorded in the presence of 4 mM $CaCl_2$, 0 $MgCl_2$, 10 μM SR-95531, and 10 mM γ-DGG at a holding potential of −40 mV. CFs were stimulated at 0.033 Hz to minimize depletion of the release-competent pool, and measurements were made from at least 20 consecutive CF EPSCs after a 10 min baseline

period. To ensure that gradual amplitude drift did not bias measurements of trial-to-trial variability, a linear fit of amplitudes was made during the sample period, and individual EPSC amplitudes were adjusted by multiplying the ratio of the raw EPSC amplitude and corresponding fit amplitude by the mean EPSC amplitude during the sample period. Because the analysis of CF mEPSCs (Fig. 4) revealed no difference in total quantal variability (CV^2) between zones (Z^+: 0.13 ± 0.01, $n = 10$; Z^-: 0.12 ± 0.01, $n = 9$; $p = 0.646$), arising from trial-to-trial variability of glutamate release from individual vesicles within or between release sites (Foster and Regehr, 2004; Clements and Silver, 2000), variance values were not corrected for quantal variability. Complex spikes were recorded at 0.05 Hz in four blocks of nine CF stimulations (single or paired); each block was briefly interrupted by switching to voltage clamp to monitor membrane and access resistance. Small hyperpolarizing currents were applied to maintain a resting potential of approximately −70 mV. Individual trials representing direct Purkinje cell stimulation were identified by the lack of delay between the stimulation artifact and onset of the initial spike component and were eliminated from analysis. All complex spike recordings were acquired within 15 min of the onset of CF stimulation. Within this period, complex spikes showed a gain or loss of, at most, one spikelet. Recordings were categorized according to the number of spikelets following the first complete spike after the stimulus. The number of spikelets per recording was determined as the average of all complex spike responses. For presentation in histograms (see Fig. 8), values were rounded to the nearest integer. In one recording from a Z^+ Purkinje cell, the complex spike consisted of multiple small wavelets riding on top of a prolonged depolarization. As it was not possible to count spikelets in this recording, this cell was only included in the analysis of the integral of the first 20 ms of the complex spike. For the experiments illustrated in Figure 8, *C* (right) and *D*, slices were preequilibrated in 10 μM DL-threo-β-benzyloxyaspartic acid (TBOA) before beginning the whole-cell recording, to minimize the duration of the complex spike recording.

All results are presented as mean ± SEM. Statistical significance was calculated using the unpaired or paired Student's *t* test or one-way ANOVA followed by Bonferroni procedures, as appropriate.

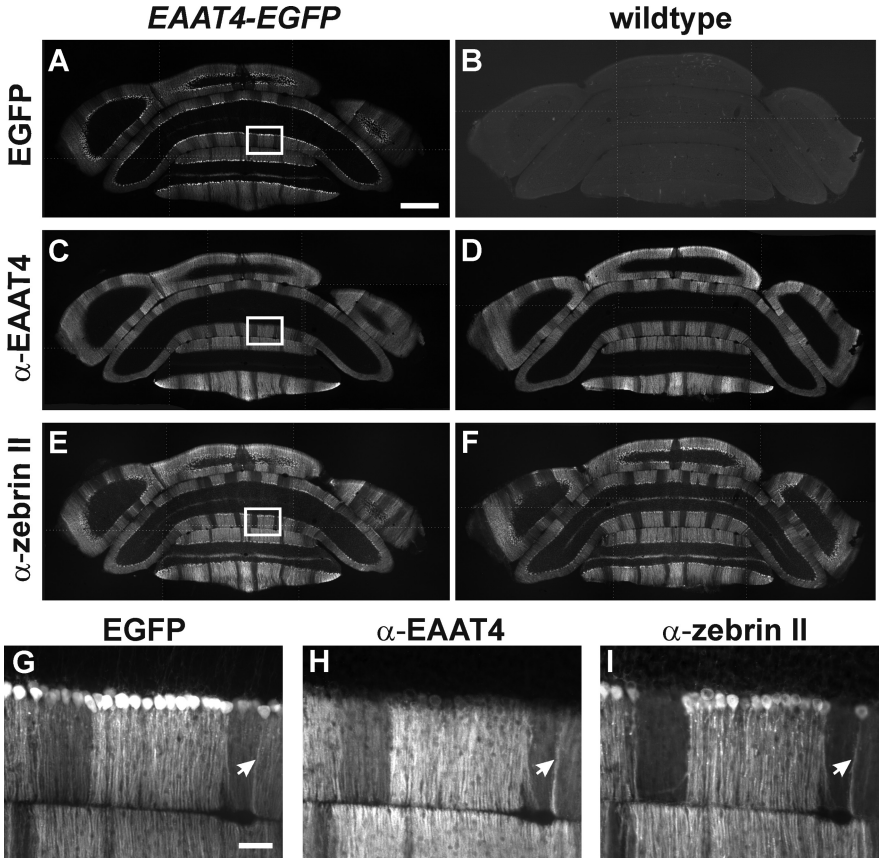

Figure 1. Parasagittal zones of Purkinje cells in *EAAT4-EGFP* mice. ***A***, ***B***, EGFP fluorescence in coronal sections of cerebella from *EAAT4-EGFP* (***A***) or wild-type (***B***) mice. ***C–F***, Sections were immunostained for EAAT4 (***C***, ***D***) and zebrin II (***E***, ***F***). The boxed areas in ***A***, ***C***, and ***E*** are shown at higher magnification in ***G–I***. Arrows highlight a single Purkinje cell that expressed high levels of EGFP, EAAT4, and zebrin II. Scale bars: ***A–F***, 500 μm; ***G–I***, 50 μm.

Results

Enhanced glutamate release from CFs in Z^+ zones prolongs Purkinje cell EPSCs

To determine whether there are differences in CF signaling between Z^+ and Z^- zones, we recorded CF responses from Purkinje cells in coronal slices of cerebellum from *EAAT4-EGFP* BAC transgenic mice, in which EGFP is expressed under the control of the EAAT4 promoter (Gincel et al., 2007). In these mice, EGFP is highly expressed by the same groups of Purkinje cells that define the EAAT4- and zebrin II-immunoreactive parasagittal bands bordering the vermis (Fig. 1), denoted $P1^+$ to $P7^+$ from the midline moving laterally (supplemental Fig. S1, available at www.jneurosci.org as supplemental material). Using EGFP as a guide, we made whole-cell voltage-clamp recordings from Purkinje cells in Z^+ ($P1^+$ and $P2^+$ bands) and Z^- ($P1^-$ band) zones within lobule VIII. Although the amplitudes of CF EPSCs between the two groups were not significantly different (Z^+: −2303 ± 99 pA, $n = 15$; Z^-: −2150 ± 78 pA, $n = 14$; $p = 0.238$) (Fig. 2*A*), CF EPSCs decayed more slowly in Z^+ than Z^- Purkinje cells (weighted decay; Z^+: 12.4 ± 0.5 ms, $n = 15$; Z^-: 9.7 ± 0.6 ms, $n = 14$; $p = 0.002$) (Fig. 2*A*). This difference in EPSC time course was not caused by variations in the desensitization rate of AMPA receptors between these groups of Purkinje cells, because the difference in decay kinetics was more pronounced when AMPA receptor desensitization was inhibited by cyclothiazide (200 μM) (Z^+: 40.8 ± 1.5 ms, $n = 9$; Z^-: 27.3 ± 2.6 ms, $n = 8$; $p < 0.001$) (Fig. 2*B*). These results suggest that glutamate remains elevated longer at CF synapses in Z^+ zones.

CFs exhibit an unusually high release probability, which causes each terminal to release multiple vesicles after invasion of an action potential and leads to saturation of AMPA receptors (Wadiche and Jahr, 2001; Foster et al., 2002). As a result of saturation, an increase in synaptic glutamate may not lead to an increase in the amplitude of CF EPSCs (Wadiche and Jahr, 2001). To provide an additional assessment of glutamate concentration at CF synapses in Z^+ and Z^- zones, we measured the inhibition of CF EPSCs by the rapidly dissociating competitive AMPA receptor antagonist γ-DGG, which becomes less effective at inhibiting AMPA receptors as the concentration of glutamate is increased (Liu et al., 1999; Wadiche and Jahr, 2001; Foster et al., 2002; Foster and Regehr, 2004). In accordance with the prolonged activation of AMPA receptors at CF synapses in Z^+ zones, CF EPSCs were inhibited less by 2 mM γ-DGG in Z^+ than in Z^- Purkinje cells (Z^+: 34 ± 5%, $n = 10$; Z^-: 45 ± 2%, $n = 10$; $p = 0.032$) (Fig. 2*C*). Together, these results indicate that more

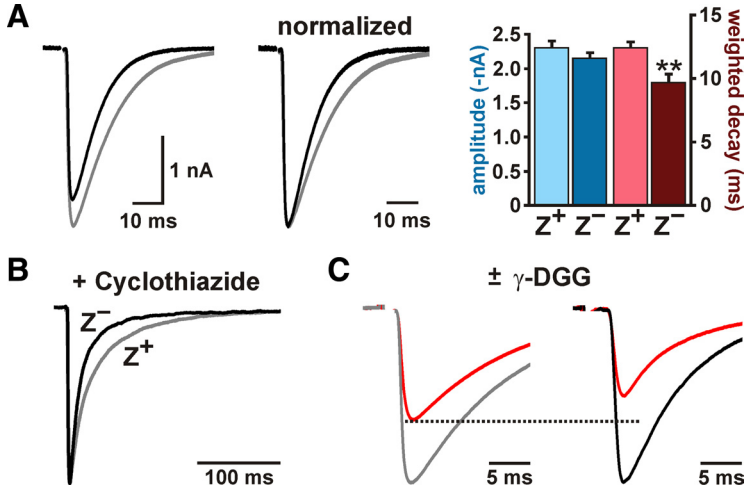

Figure 2. CFs that innervate Z^+ Purkinje cells elicit prolonged EPSCs as a result of enhanced glutamate release. ***A***, CF EPSCs from representative Z^+ (gray trace) or Z^- (black trace) Purkinje cells. Traces at right were normalized to the peak amplitude. Histograms show the peak amplitude and weighted decay of CF EPSCs from Z^+ ($n = 15$) and Z^- ($n = 14$) Purkinje cells (**$p < 0.01$). ***B***, Representative average CF EPSCs recorded from Z^+ (gray trace) and Z^- (black trace) Purkinje cells in the presence of 200 μM cyclothiazide. Responses have been normalized to the peak amplitude. ***C***, Average CF EPSCs recorded in the presence or absence of 2 mM γ-DGG from a Z^+ (gray trace) and a Z^- (black trace) Purkinje cell.

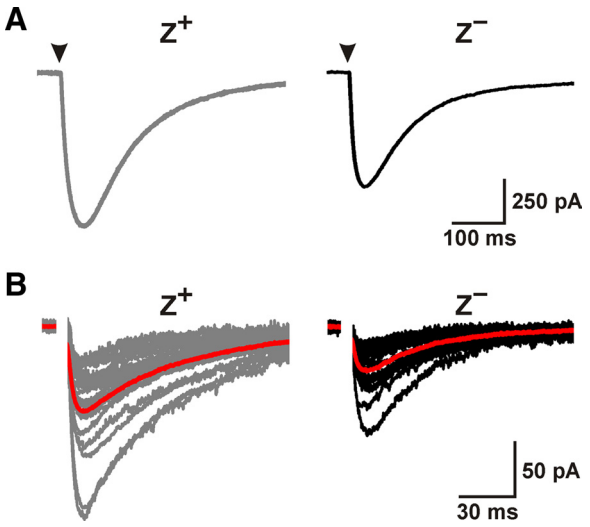

Figure 3. Purkinje cells in Z^+ zones exhibit larger glutamate transporter currents. ***A***, EAAT4-mediated transporter currents elicited through photolysis of MNI-D-aspartate recorded from Z^+ (gray trace) or Z^- (black trace) Purkinje cells ($V_m = -70$ mV). Arrowheads indicate the onset of 1 ms UV exposure. ***B***, CF-evoked transporter currents recorded from Z^+ or Z^- Purkinje cells ($V_m = -70$ mV). Red traces represent average responses.

glutamate is released per action potential from each CF in Z^+ zones.

CF synapses in Z^+ zones contain more EAAT4 but exhibit delayed glutamate clearance

Glutamate transporters such as EAAT4 shape the spatial and temporal profile of glutamate near receptors and can influence the amplitude and time course of synaptic currents (Brasnjo and Otis, 2001; Takayasu et al., 2005; Wadiche and Jahr, 2005). The higher EAAT4 immunoreactivity in Z^+ zones suggests that glutamate clearance should be more rapid in these regions; however, CF EPSCs decayed more slowly in these zones, indicating that glutamate transients at these synapses were more prolonged. To address whether the increased EAAT4 expression in Z^+ zones translates into a larger number of functional transporters, we recorded glutamate transporter currents from Purkinje cells induced by photolysis of MNI-D-aspartate (Huang et al., 2005). Because EAAT4 is exclusively responsible for transporter currents in Purkinje cells (supplemental Fig. S2, available at www.jneurosci.org as supplemental material) (Huang et al., 2004), the amplitude of these responses is proportional to the number of EAAT4 transporters. Photolysis-evoked transporter currents were significantly larger in Z^+ than in Z^- Purkinje cells (Z^+: -906 ± 77 pA, $n = 16$; Z^-: -616 ± 76 pA, $n = 15$; $p = 0.012$) (Fig. 3*A*), indicating that increased EAAT4 promoter activity is translated into a higher surface expression of EAAT4. In accordance with evidence of enhanced glutamate release from CFs in Z^+ zones, CF-induced transporter currents in Purkinje cells were also larger in these regions (Z^+: -75 ± 8 pA, $n = 21$; Z^-: -39 ± 5 pA, $n = 18$; $p < 0.001$) (Fig. 3*B*), suggesting that more glutamate transporters were activated at these synapses.

CFs exhibit enhanced multivesicular release in Z^+ zones

The higher glutamate concentration at CF synapses in Z^+ zones could result from release of vesicles loaded with more glutamate or from enhanced multivesicular release (Wadiche and Jahr, 2001). To test the former possibility, we examined the amplitude and time course of mEPSCs, which were evoked from CFs after replacing extracellular Ca^{2+} with Sr^{2+} (Miledi, 1966; Oliet et al., 1996; Xu-Friedman and Regehr, 2000). The amplitude (Z^+: -31 ± 2 pA, $n = 10$; Z^-: -30 ± 1 pA; $n = 9$; $p = 0.506$) and decay time course (tau decay; Z^+: 4.8 ± 0.3 ms, $n = 10$; Z^-: 4.3 ± 0.4 ms, $n = 8$; $p = 0.271$) of mEPSCs were similar between Purkinje cells in the two zones (Fig. 4), suggesting that vesicles in these terminals contain comparable amounts of glutamate.

When repetitive stimuli are applied to CFs, γ-DGG is more effective at inhibiting successive EPSCs, because of a reduction in multivesicular release through slow replenishment of the release-competent vesicle pool (Wadiche and Jahr, 2001; Foster and Regehr, 2004). We took advantage of this phenomenon to assess whether multivesicular release varies between Z^+ and Z^- zones. To increase the sensitivity of this assay, we reduced release probability using 0.5 mM Ca^{2+} and 3.3 mM of Mg^{2+} in the external solution (see Materials and Methods). If CF multivesicular release were similar in Z^+ and Z^- zones, the PPR (EPSC2/EPSC1) should be altered to the same extent by γ-DGG. However, the PPR of CF EPSCs in Z^+ Purkinje cells was reduced $14 \pm 3\%$ by γ-DGG ($n = 11$) and in Z^- Purkinje cells by only $3 \pm 2\%$ ($n = 10$; $p = 0.012$) (Fig. 5*A*,*B*). In contrast, the high-affinity AMPA receptor antagonist NBQX, which should remain bound during each synaptic event, inhibited CF EPSCs in Z^+ and Z^- Purkinje cells by the same amount (Z^+: $69 \pm 2\%$, $n = 9$; Z^-: $72 \pm 2\%$, $n = 9$; $p = 0.4$) (Fig. 5*C*) and did not differentially alter the PPR (Z^+: $7 \pm 1\%$, $n = 8$; Z^-: $7 \pm 2\%$, $n = 9$; $p = 0.903$) (Fig. 5*D*). These results support the hypothesis that the prolonged time course of CF EPSCs in Z^+ zones is attributable to enhanced multivesicular release.

CF terminals in Z$^+$ zones have a larger pool of release-ready vesicles

Greater multivesicular release could originate either from a larger pool of release-ready vesicles, or from an enhancement in the release probability of individual vesicles (P_v). To distinguish between these two possibilities, we performed variance–mean analysis of CF EPSCs recorded from Purkinje cells in the two zones. Under experimental conditions in which P_v is larger than 0.5 but smaller than 1, and AMPA receptors are relieved from saturation by γ-DGG, the mean EPSC amplitude is expected to be larger in Z$^+$ Purkinje cells when the pool size is larger or P_v is higher; however, the accompanying trial-to-trial variability in EPSC amplitude would be larger in the former case but smaller in the latter case (Clements and Silver, 2000). Analysis of mean amplitude and variance of CF EPSCs in the presence of γ-DGG (10 mM) and elevated Ca^{2+} (4 mM), which should result in P_v safely larger than 0.5 (Foster and Regehr, 2004), revealed that CF EPSCs in Z$^+$ Purkinje cells had larger mean amplitudes (Z$^+$: −1372 ± 165 pA, $n = 9$; Z$^-$: −836 ± 115 pA, $n = 8$; $p = 0.020$) and exhibited higher variance (Z$^+$: 1012 ± 178 pA^2, $n = 9$; Z$^-$: 430 ± 114 pA^2, $n = 8$; $p = 0.018$) (Fig. 6), suggesting that CF terminals in Z$^+$ zones contain a larger pool of release-competent vesicles.

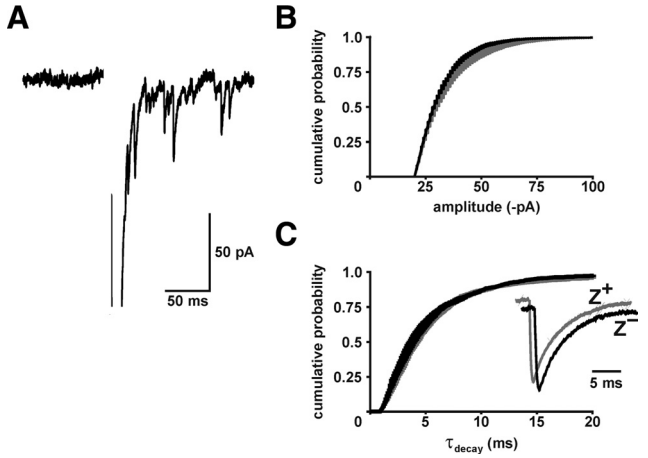

Figure 4. CF synaptic vesicles in Z$^+$ and Z$^-$ zones contain a similar amount of glutamate. ***A***, CF-induced mEPSCs recorded in the presence of $SrCl_2$ ($V_m = -70$ mV). ***B***, ***C***, Average amplitude (Z$^+$: 17,792 events, $n = 10$; Z$^-$: 6705 events, $n = 9$) and decay time (tau decay; Z$^+$: 5520 events, $n = 10$; Z$^-$: 1731 events, $n = 8$) of CF-evoked mEPSCs from Z$^+$ and Z$^-$ Purkinje cells (mean ± SEM). The inset shows averaged scaled CF mEPSCs from representative Z$^+$ (gray) and Z$^-$ (black) Purkinje cells.

The two excitatory projections to the cerebellar cortex use distinct vesicular transporters to load synaptic vesicles with glutamate; parallel fibers rely on vGluT1, whereas CFs use vGluT2 (Fremeau et al., 2001), providing a means to examine these different pools of synaptic vesicles histologically. Analysis of the molecular layer in sections of cerebellum revealed that Z$^+$ zones exhibited enhanced vGluT2 immunoreactivity (Fig. 7*A*,*B*). Indeed, when a threshold was applied to include the largest 5% of pixel values in Z$^+$ zones, only 3.1 ± 0.2% of Z$^-$ pixel values remained suprathreshold in these sections ($n = 19$ sections from five mice; $p < 0.001$) (Fig. 7*C*). Similar differences in vGluT2 immunoreactivity were observed in the cerebellum of rats (supplemental Fig. S3, available at www.jneurosci.org as supplemental material), which exhibit a similar pattern of EAAT4 and zebrin II expression. This increase in vGluT2 immunoreactivity could reflect a larger number of transporters per vesicle or a larger number of vesicles. Enhanced vGluT expression can lead to an increase in quantal size (Wilson et al., 2005; Moechars et al., 2006); however, because quantal size was similar at CF synapses in Z$^+$ and Z$^-$ zones (Fig. 4), these results provide additional support for the conclusion that CFs in Z$^+$ zones contain a larger pool of release-competent vesicles.

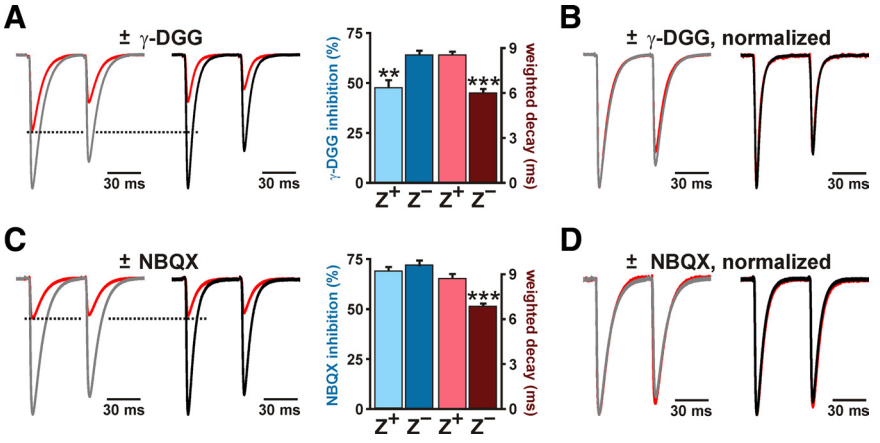

Figure 5. CFs in Z$^+$ zones exhibit enhanced multivesicular release. ***A***, CF EPSCs elicited through paired stimulation in the presence or absence of 1 mM γ-DGG (red trace; ± γ-DGG) from representative Z$^+$ (gray) and Z$^-$ (black) Purkinje cells. Responses are normalized to peak of EPSC1. The histogram shows percentage inhibition and weighted decay of EPSC1 for Z$^+$ ($n = 11$) and Z$^-$ ($n = 10$) Purkinje cells (**$p < 0.01$; ***$p < 0.001$). ***B***, CF EPSCs in 1 mM γ-DGG normalized to the first peak in the absence of γ-DGG. ***C***, CF EPSCs recorded as described in ***A***; however, red traces show responses recorded in 120 nM NBQX. The histogram at right shows the inhibition by NBQX and the weighted decay for the first CF EPSC in Z$^+$ ($n = 9$) and Z$^-$ ($n = 9$) Purkinje cells (mean ± SEM; ***$p < 0.001$). ***D***, CF EPSCs recorded in the presence or absence of NBQX in ***C*** normalized to the peak amplitude of the first response. In all panels, recordings were performed in ACSF containing 0.5 mM $CaCl_2$ and 3.3 mM $MgCl_2$.

EAAT4 does not impact glutamate release from CFs, and CFs do not regulate EAAT4 expression

To determine whether EAAT4 contributes to the difference in CF EPSC time course between Z$^+$ and Z$^-$ zones, we bred *EAAT4*$^{-/-}$ mice to *EAAT4-EGFP* mice and compared the time course of CF EPSCs in these animals to CF EPSCs in animals that had a normal complement of EAAT4. In *EAAT4*$^{-/-}$; *EAAT4-EGFP* mice, both the nonuniform EAAT4 promoter activity and the nonuniform expression of zebrin II were preserved in the absence of EAAT4, as indicated by the appropriate banded expression pattern of EGFP and zebrin II in these mice (supplemental Fig. S4*A*, available at www.jneurosci.org as supplemental material). Moreover, CF EPSCs recorded from Purkinje cells in Z$^+$ and Z$^-$ zones in *EAAT4*$^{-/-}$ mice decayed at the same rate as EPSCs in Z$^+$ and Z$^-$ Purkinje cells that had the normal amount of EAAT4 (*EAAT4*$^{-/-}$, Z$^+$: 12.4 ± 0.4 ms, $n = 8$, $p > 0.9$; *EAAT4*$^{-/-}$, Z$^-$: 8.5 ± 0.6 ms, $n = 8$, $p > 0.9$; *EAAT4*$^{-/-}$, Z$^+$ vs *EAAT4*$^{-/-}$, Z$^-$: $p < 0.005$) (supplemental Fig. S4*B*, available at www.jneurosci.org as supplemental material). These results indicate that the differences in glutamate release from CFs are established and maintained independent of EAAT4 and support the conclusion that differences in synaptic glutamate levels between Z$^+$ and Z$^-$ zones arise from presynaptic changes in CFs rather than postsynaptic changes in EAAT4 activity.

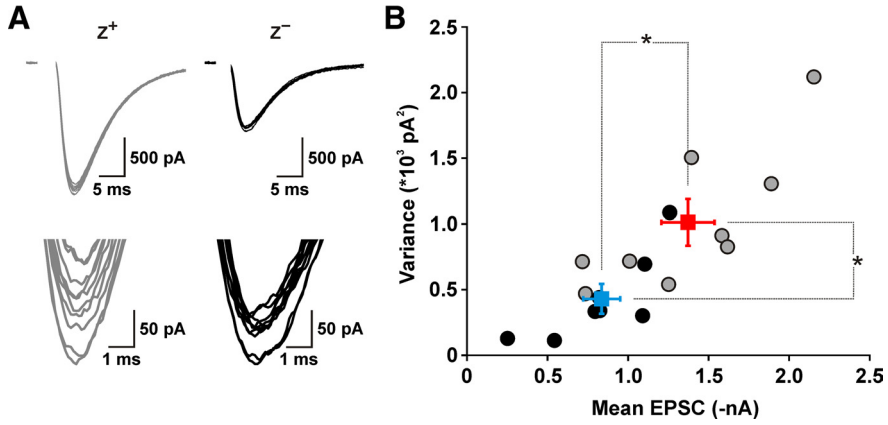

Figure 6. CFs in Z^+ zones contain a larger pool of release-competent vesicles. ***A***, Top, Overlay of 10 consecutive EPSCs from representative Z^+ (gray traces) and Z^- (black traces) Purkinje cells collected at 0.033 Hz in 4 mM extracellular Ca^{2+} in the presence of 10 mM γ-DGG (to relieve AMPA receptors from saturation). Recordings were made at a holding potential of −40 mV. Bottom, Same traces presented at an enlarged scale. ***B***, Graph of variance versus mean EPSC amplitude calculated from at least 20 consecutive CF EPSCs. CF responses in Z^+ zones (red symbols) exhibited larger amplitudes ($p = 0.02$) and higher variance ($p < 0.02$) than CF responses in Z^- zones (blue symbols), indicating that CFs in Z^+ zones contain a larger pool of release-competent vesicles. Squares and error bars represent mean ± SEM.

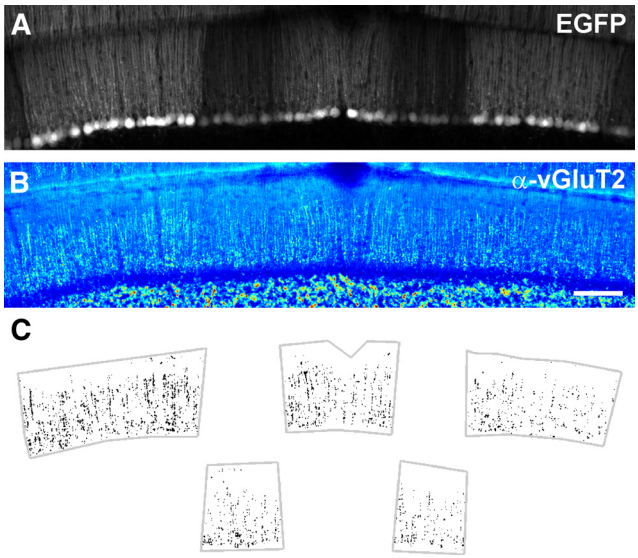

Figure 7. CFs in Z^+ zones exhibit higher vGluT2 immunoreactivity. ***A***, Native EGFP fluorescence in a coronal section of cerebellum from an *EAAT4-EGFP* mouse containing Z^+ and Z^- zones. ***B***, vGluT2 immunoreactivity for the region shown in ***A***, pseudocolored with warmer colors indicating higher pixel intensities. Scale bar, 100 μm. ***C***, Plot of all pixels in Z^+ (top) and Z^- (bottom) zones from the section shown in ***A*** that exceeded a threshold set at 95% of pixel intensities measured within Z^+ zones.

Glutamate transporter expression can be regulated by neuronal activity (Yang et al., 2009), raising the possibility that the increase in EAAT4 in Z^+ zones represents an adaptation to the enhanced glutamate release by the groups of CFs that project to these regions. To determine whether CFs are required to maintain the nonuniform pattern of EAAT4 expression, we ablated CF axons *in vivo* using a combination of 3-acetylpyridine (3-AP), harmaline, and nicotinamide, which destroys projection neurons in the IO (Llinas et al., 1975; O'Hearn and Molliver, 1997). As this procedure is less effective in mice, these studies were performed in rats. Four weeks after this treatment, most large neurons in the IO were absent (supplemental Fig. S5*A*,*B*,*F*,*G*, available at www.jneurosci.org as supplemental material), and vGluT2 immunoreactivity in the molecular layer of the cerebellum was absent (supplemental Fig. S5*C*,*H*, available at www.jneurosci.org as supplemental material). Similar results were observed after only 1 week following treatment (data not shown), indicating that Purkinje cells in these animals had been devoid of CF innervation for at least 3 weeks. Nevertheless, the patterned expression of both EAAT4 and zebrin II were maintained (supplemental Fig.S5 *D*,*E*,*I*,*J*, available at www.jneurosci.org as supplemental material), although there was a small reduction in the ratio of mean pixel intensity (Z^+/Z^-) between zones (EAAT4, control: 1.87 ± 0.03, $n = 10$ sections from four rats; 3-AP: 1.78 ± 0.03, $n = 15$ sections from six rats, $p = 0.049$; zebrin II, control: 1.96 ± 0.04, $n = 10$ sections from four rats, 3-AP: 1.80 ± 0.03, 15 sections from six rats, $p = 0.004$). These results suggest that CFs do not regulate the expression of EAAT4 or zebrin II by Purkinje cells.

CF-induced complex spikes are prolonged in Z^+ Purkinje cells

The summed activity of the hundreds of synapses formed by each CF triggers a complex spike in Purkinje cells consisting of a single action potential followed by a series of spikelets of smaller amplitude (Eccles et al., 1966). The duration of the CF-induced depolarization and the number of spikelets present in each complex spike varies among Purkinje cells (Khaliq and Raman, 2005) and is strongly influenced by the magnitude of the CF-induced conductance change (Foster et al., 2002; Davie et al., 2008). To evaluate whether the difference in EPSC time course between Z^+ and Z^- zones affects the shape of the complex spike, we compared CF-induced depolarizations from Purkinje cells in these two zones. Complex spikes recorded from Z^+ and Z^- Purkinje cells contained one to three spikelets, and complex spike waveforms were consistent within individual cells (Fig. 8*A*). However, complex spikes in Z^+ Purkinje cells contained a larger number of spikelets (Z^+: 1.9 ± 0.2, $n = 11$; Z^-: 1.3 ± 0.1, $n = 13$; $p = 0.031$) (Fig. 8*B*), which was also evident when comparing the integral of the first 20 ms of the complex spike (Z^+: 396 ± 17 mV · ms, $n = 12$; Z^-: 275 ± 12 mV · ms, $n = 13$; $p < 0.001$). These results raise the possibility that prolonged activation of AMPA receptors in Z^+ Purkinje cells leads to enhanced excitation.

To determine whether differences in EPSC duration are responsible for the variations in complex spike waveform, we slowed the decay of CF EPSCs in Z^- Purkinje cells with TBOA, an antagonist of neuronal and glial glutamate transporters (Fig. 8*C*). In TBOA (10 μM), the decay time of CF EPSCs in Z^- Purkinje cells increased from 8.9 ± 0.5 ms ($n = 7$) to 11.0 ± 0.5 ms ($n = 7$; $p = 0.012$), approaching the decay time of CF EPSCs in Z^+ Purkinje cells. Under these conditions, complex spikes in Z^- Purkinje cells contained the same number of spikelets (Z^- in TBOA: 1.9 ± 0.2, $n = 12$; $p = 0.973$) and had the same integral (362 ± 27 mV · ms; $n = 12$; $p = 0.305$) as complex spikes recorded from Z^+ Purkinje cells (Fig. 8*D*). These results indicate that lower synaptic glutamate levels are sufficient to account for shorter-duration complex spikes in Z^- Purkinje cells and that Purkinje cells within Z^+ bands experience greater excitation from the IO.

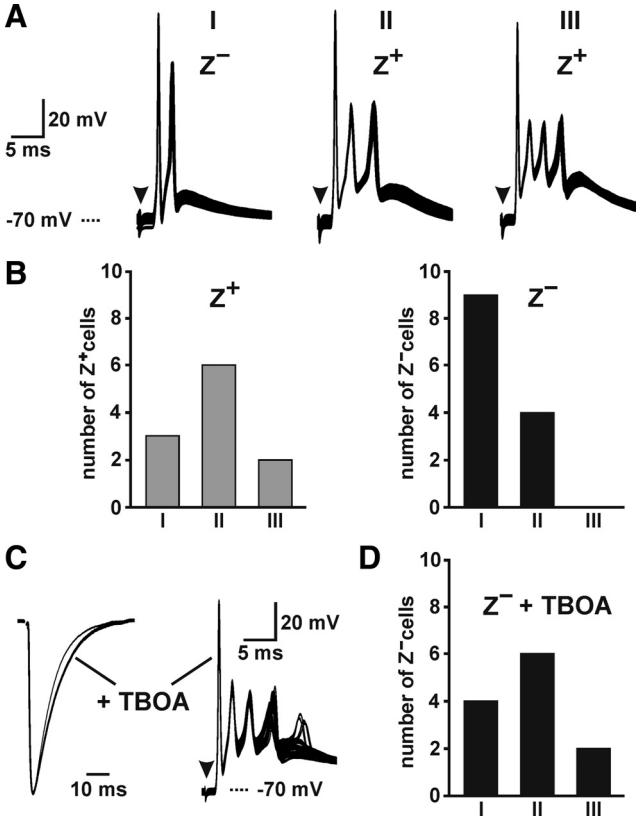

Figure 8. Increased dynamic range of CF-induced complex spikes in Z^+ Purkinje cells. ***A***, CF-evoked complex spikes in Purkinje cells contained one to three spikelets (26–33 consecutive trials shown). ***B***, Histograms showing the number of Purkinje cells in Z^+ and Z^- zones that exhibited complex spikes containing one to three spikelets. ***C***, CF EPSCs with or without TBOA (left) and complex spikes plus TBOA (right) recorded from two Z^- Purkinje cells (5 of 34 consecutive responses showed 4 spikelets). ***D***, Histogram showing the number of Z^- Purkinje cells that exhibited complex spikes containing one to three spikelets in TBOA (10 μM).

Discussion

The mammalian cerebellum is organized into a series of parasagittal zones consisting of molecularly distinct Purkinje cells that are innervated by separate groups of CFs. To determine whether CFs that project to these different zones exhibit distinct physiological properties, we recorded CF responses from Purkinje cells in acute cerebellar slices from transgenic mice in which these zones can be visualized. Our studies indicate that CFs that innervate Purkinje cells in Z^+ zones release more glutamate per action potential, which prolongs AMPA receptor-mediated EPSCs and triggers longer-duration complex spikes. These results indicate that the parasagittal organization of the cerebellum is defined not only by molecular phenotype of Purkinje cells within zones, but also by the physiological properties of CFs that project to these distinct regions.

EAAT4-EGFP mice allow functional analysis of signaling in zebrin zones

Although the cellular composition and local circuit organization of the cerebellar cortex is remarkably similar across all folia, Purkinje cells exhibit regional differences in gene expression. Purkinje cells that express high levels of the glutamate transporter EAAT4 and the glycolytic enzyme zebrin II (aldolase C) cluster in zones or bands that extend through the cerebellum in the longitudinal (rostrocaudal) orientation. Purkinje cells within these distinct zones receive CF input from discrete regions of the IO, raising the possibility that these molecular differences between Purkinje cells reflect the physiological properties or patterns of activity exhibited by different groups of CFs. Although Z^+ and Z^- zones are highly reproducible between animals, it has been difficult to compare the physiological properties of these projections, because of the challenges associated with reliably identifying Purkinje cells within different zones in living tissue. Here we used *EAAT4-EGFP* mice (Gincel et al., 2007) to identify and record CF responses in Purkinje cells in defined zones within the same folia. We found that EGFP expression in these mice is elevated in the same groups of Purkinje cells that exhibited enhanced expression of EAAT4 and zebrin II and that Z^+ and Z^- Purkinje cells could be distinguished with single-cell resolution in acute cerebellar slices, providing unprecedented access to this highly conserved aspect of cerebellar organization.

Enhanced glutamate release from CFs in Z^+ zones prolongs Purkinje cell EPSCs

Our studies indicate that CFs within Z^+ zones release more glutamate per action potential than CFs in Z^- zones, which leads to prolonged EPSCs in Purkinje cells in Z^+ regions. The conclusion that glutamate release varies among these distinct groups of olivo-cerebellar projections is supported by several independent lines of evidence. CF EPSCs in Z^+ Purkinje cells decayed more slowly, exhibited larger amplitudes when AMPA receptor saturation was removed, and were less sensitive to the rapidly dissociating competitive AMPA receptor antagonist γ-DGG. The PPR of CF EPSCs in Z^+ zones was reduced more by γ-DGG, as expected if multivesicular release was enhanced in these regions (Wadiche and Jahr, 2001), and variance–mean analysis of CF EPSCs under nonsaturating conditions indicated that CFs in Z^+ zones contain a larger pool of release-competent vesicles. In addition, CF-induced mEPSCs were similar between the two zones, consistent with a presynaptic locus for the change in EPSC time course. While there have been no reports of structural differences between CF synapses in Z^+ and Z^- zones, we found that vGluT2 immunoreactivity was higher within Z^+ zones in the cerebella of both rat and mouse, consistent with a larger number of synaptic vesicles. Although these results indicate that individual CF terminals in Z^+ zones release more glutamate, it is possible that other differences, such as an increase in the number of CF–Purkinje cell synapses, could also contribute to the enhanced CF EPSCs in these regions.

In a previous study using acute slices of rat cerebellum (Wadiche and Jahr, 2005), CF signaling was compared between Purkinje cells located in lobule X, a region where the majority of Purkinje cells are zebrin II^+ and express elevated EAAT4, and lobule III, where the majority are zebrin II^- and express lower levels of EAAT4 (Ozol et al., 1999). In contrast to our findings, the amount of block of CF EPSCs by γ-DGG was similar between Purkinje cells in these different lobules. Although we did not compare CF EPSCs between these particular regions of the cerebellum in *EAAT4-EGFP* mice, differences in CF glutamate release between Z^+ and Z^- Purkinje cells may have been larger in our study, as we selected Purkinje cells that exhibited the greatest and least EGFP fluorescence within zones for recordings. An additional possibility is that differences in CF glutamate release may only be apparent when comparing CF synapses in adjacent zebrin bands. Such local differences in CF signaling could enhance contrast and facilitate partitioning of information from similar sensory modalities. In this scenario, Z^+ and Z^- Purkinje cells in different lobules may not differ in the absolute levels of glutamate release from CFs.

EAAT4 function at CF synapses

Glutamate transporters are essential components of excitatory, glutamatergic synapses in the CNS; they remove glutamate released during synaptic transmission, terminating its action and preventing accumulation that would otherwise disrupt signaling, and they shape the activation of receptors by influencing the time course and spatial spread of glutamate (Huang and Bergles, 2004). EAAT4 is expressed exclusively by Purkinje cells, where it is enriched in perisynaptic membranes at CF and parallel fiber synapses (Dehnes et al., 1998). Although release of glutamate from CFs elicits transporter-mediated currents in Purkinje cells (Otis et al., 1997; Auger and Attwell, 2000) (Fig. 3*B*), indicating that these transporters are positioned near CF terminals, they remove only a small fraction (<10%) of the glutamate released per action potential (Brasnjo and Otis, 2004; Huang et al., 2004). In accordance with these findings, the decay kinetics of CF EPSCs in both Z^+ and Z^- zones were unaltered in EAAT4 null mice (supplemental Fig. S4*B*, available at www.jneurosci.org as supplemental material), indicating that these transporters do not influence the profile of glutamate sensed by AMPA receptors at CF synapses and that other transporter-mediated effects, such as transmitter buffering, do not account for the delayed clearance of glutamate from CF synapses in Z^+ zones. Nevertheless, previous studies have shown that CF EPSCs in some Purkinje cells in EAAT4 null mice exhibit a long-lasting tail current (Takayasu et al., 2005), suggesting that EAAT4 can influence AMPA receptor activation. However, the incidence of prolonged CF EPSCs was low among Purkinje cells (<30%) at the ages studied here (P21 or younger) (Takayasu et al., 2005), and it is unknown whether these neurons occur in the regions of the cerebellum examined here. Although previous studies indicate that glutamate transporter currents in Purkinje cells can be rapidly potentiated by tetanic stimulation of CFs (Shen and Linden, 2005), ablation of CFs did not alter the differential expression of EAAT4 between Z^+ and Z^- zones (supplemental Fig. 5, available at www.jneurosci.org as supplemental material), indicating that regional variations in EAAT4 expression are unlikely to result from differences in CF activity.

The metabotropic glutamate receptor 1 (mGluR1) is localized to the same perisynaptic domains that contain EAAT4 (Nusser et al., 1994; Dehnes et al., 1998). Selective inhibition of glutamate uptake into Purkinje cells enhances activation of mGluRs (Brasnjo and Otis, 2001), and parallel fiber-induced, mGluR-mediated currents are larger and exhibit faster kinetics in mice that lack EAAT4 (Nikkuni et al., 2007). Consistent with these findings, parallel fiber-mediated mGluR responses are smaller for a given stimulus in Purkinje cells located in lobule X than in lobule III (Wadiche and Jahr, 2005). Together, these results indicate that EAAT4 influences glutamate dynamics in the region outside parallel fiber synapses and shapes the activation of mGluRs. Glutamate release from CFs can also trigger mGluR activation in some Purkinje cells, and this component of CF EPSCs is dramatically enhanced when glutamate transporters are inhibited (Dzubay and Otis, 2002). The higher EAAT4 expression by Purkinje cells in Z^+ zones may help prevent excessive mGluR1 activation, as well as enhanced spillover of glutamate to surrounding parallel fiber synapses, interneurons (Szapiro and Barbour, 2007), and Bergmann glial cells (Bergles et al., 1997; Clark and Barbour, 1997).

Physiological impact of differential glutamate release from CFs among zebrin zones

CF-mediated excitation of Purkinje cells leads to the generation of a complex spike, a prolonged depolarization consisting of a single action potential followed by a series of smaller spikelets (Eccles et al., 1966). In accordance with the slower decay of CF EPSCs in Z^+ zones, Purkinje cells in these regions also exhibited longer complex spikes containing more spikelets. Previous studies have shown that the shape of complex spikes is dependent on the strength of CF input (Coesmans et al., 2004; Carey and Regehr, 2009; Mathy et al., 2009). Indeed, prolonging CF EPSCs in Z^- Purkinje cells by impairing glutamate uptake was sufficient to mimic the extended time course of complex spikes in Z^+ Purkinje cells (Fig. 8*C*,*D*), suggesting that the differences in complex spike waveform are unlikely to arise from other phenotypic differences between these groups of Purkinje cells. Elevated expression of the glycolytic enzyme aldolase C in Z^+ zones may help compensate for enhanced CF-mediated excitation of Purkinje cells in these regions.

Purkinje cells within Z^+ and Z^- zones exhibit synchronized activity (Sugihara et al., 2007), a consequence of the restricted arborization of CFs within zones (Sugihara et al., 2001) and concerted activity of groups of neurons in the IO that give rise to these axons (Llinas et al., 1974; Sugihara et al., 2007). The prolonged CF-induced depolarization of Purkinje neurons in Z^+ zones should enhance Ca^{2+} influx, which could facilitate activity-dependent changes in the strength of CF and parallel fiber synapses (Hansel et al., 2001; Safo et al., 2006; Carey and Regehr, 2009; Mathy et al., 2009). However, these forms of plasticity rely on activation of mGluRs. As EAAT4 controls how much glutamate is available to bind to perisynaptic mGluRs (Wadiche and Jahr, 2005; Wadiche et al., 2006; Nikkuni et al., 2007), enhanced expression of EAAT4 in Z^+ zones may help bring parity among Z^+ and Z^- zones for induction of mGluR-dependent plasticity.

Purkinje cells convey their activity to projection neurons residing in DCN, which provide the primary output of the cerebellum. Purkinje cell–DCN synapses are able to sustain high rates of activity by forming boutons that contain multiple release sites, where transmitter spillover can minimize the depressive effects of vesicle depletion (Telgkamp et al., 2004). High-frequency Purkinje cell activity induces repetitive release of GABA at these Purkinje cell–DCN synapses and temporarily halts the spontaneous firing of DCN neurons (Telgkamp and Raman, 2002; Alvina et al., 2008). Unlike trains of somatic action potentials, only 30% of first spikelets and ~60% of subsequent spikelets are transmitted as action potentials to the DCN (Khaliq and Raman, 2005; Monsivais et al., 2005). Our findings suggest that Z^+ Purkinje cells are more likely to transmit a high-frequency burst of action potentials during a complex spike and silence DCN neurons for longer periods.

Purkinje cells within longitudinal zones project to discrete regions of the DCN (Sugihara et al., 2009), and there is a high degree of convergence of Purkinje cells onto DCN neurons (Palkovits et al., 1977). As CFs within zones exhibit synchronized activity (Sugihara et al., 2007), any differences in Purkinje cell activity among zones are likely to be mirrored by corresponding areas of the DCN. The partitioning of identical sensory information through separate cortico-nuclear compartments at differential gain may be advantageous for cerebellar processing.

References

Alvina K, Walter JT, Kohn A, Ellis-Davies G, Khodakhah K (2008) Questioning the role of rebound firing in the cerebellum. Nat Neurosci 11:1256–1258.

Auger C, Attwell D (2000) Fast removal of synaptic glutamate by postsynaptic transporters. Neuron 28:547–558.

Bergles DE, Dzubay JA, Jahr CE (1997) Glutamate transporter currents in Bergmann glial cells follow the time course of extrasynaptic glutamate. Proc Natl Acad Sci U S A 94:14821–14825.

Blenkinsop TA, Lang EJ (2006) Block of inferior olive gap junctional coupling decreases Purkinje cell complex spike synchrony and rhythmicity. J Neurosci 26:1739–1748.

Brasnjo G, Otis TS (2001) Neuronal glutamate transporters control activation of postsynaptic metabotropic glutamate receptors and influence cerebellar long-term depression. Neuron 31:607–616.

Brasnjo G, Otis TS (2004) Isolation of glutamate transport-coupled charge flux and estimation of glutamate uptake at the climbing fiber-Purkinje cell synapse. Proc Natl Acad Sci U S A 101:6273–6278.

Brenowitz SD, Regehr WG (2005) Associative short-term synaptic plasticity mediated by endocannabinoids. Neuron 45:419–431.

Brochu G, Maler L, Hawkes R (1990) Zebrin II: a polypeptide antigen expressed selectively by Purkinje cells reveals compartments in rat and fish cerebellum. J Comp Neurol 291:538–552.

Carey MR, Regehr WG (2009) Noradrenergic control of associative synaptic plasticity by selective modulation of instructive signals. Neuron 62:112–122.

Clark BA, Barbour B (1997) Currents evoked in Bergmann glial cells by parallel fibre stimulation in rat cerebellar slices. J Physiol 502:335–350.

Clements JD, Silver RA (2000) Unveiling synaptic plasticity: a new graphical and analytical approach. Trends Neurosci 23:105–113.

Coesmans M, Weber JT, De Zeeuw CI, Hansel C (2004) Bidirectional parallel fiber plasticity in the cerebellum under climbing fiber control. Neuron 44:691–700.

Davie JT, Clark BA, Häusser M (2008) The origin of the complex spike in cerebellar Purkinje cells. J Neurosci 28:7599–7609.

Dehnes Y, Chaudhry FA, Ullensvang K, Lehre KP, Storm-Mathisen J, Danbolt NC (1998) The glutamate transporter EAAT4 in rat cerebellar Purkinje cells: a glutamate-gated chloride channel concentrated near the synapse in parts of the dendritic membrane facing astroglia. J Neurosci 18:3606–3619.

Dzubay JA, Otis TS (2002) Climbing fiber activation of metabotropic glutamate receptors on cerebellar Purkinje neurons. Neuron 36:1159–1167.

Eccles JC, Llinas R, Sasaki K (1966) The excitatory synaptic action of climbing fibres on the Purkinje cells of the cerebellum. J Physiol 182:268–296.

Foster KA, Regehr WG (2004) Variance-mean analysis in the presence of a rapid antagonist indicates vesicle depletion underlies depression at the climbing fiber synapse. Neuron 43:119–131.

Foster KA, Kreitzer AC, Regehr WG (2002) Interaction of postsynaptic receptor saturation with presynaptic mechanisms produce a reliable synapse. Neuron 36:1115–1126.

Fremeau Jr RT, Troyer MD, Pahner I, Nygaard GO, Tran CH, Reimer RJ, Bellocchio EE, Fortin D, Storm-Mathisen J, Edwards RH (2001) The expression of vesicular glutamate transporters defines two classes of excitatory synapse. Neuron 31:247–260.

Gao W, Chen G, Reinert KC, Ebner TJ (2006) Cerebellar cortical molecular layer inhibition is organized in parasagittal zones. J Neurosci 26: 8377–8387.

Gincel D, Regan MR, Jin L, Watkins AM, Bergles DE, Rothstein JD (2007) Analysis of cerebellar Purkinje cells using EAAT4 glutamate transporter promoter reporter in mice generated via bacterial artificial chromosome-mediated transgenesis. Exp Neurol 203:205–212.

Hansel C, Linden DJ, D'Angelo E (2001) Beyond parallel fiber LTD: the diversity of synaptic and non-synaptic plasticity in the cerebellum. Nat Neurosci 4:467–475.

Hawkes R, Gravel C (1991) The modular cerebellum. Prog Neurobiol 36:309–327.

Huang YH, Bergles DE (2004) Glutamate transporters bring competition to the synapse. Curr Opin Neurobiol 14:346–352.

Huang YH, Dykes-Hoberg M, Tanaka K, Rothstein JD, Bergles DE (2004) Climbing fiber activation of EAAT4 transporters and kainate receptors in cerebellar Purkinje cells. J Neurosci 24:103–111.

Huang YH, Sinha SR, Fedoryak OD, Ellis-Davies GC, Bergles DE (2005) Synthesis and characterization of 4-methoxy-7-nitroindolinyl-D-aspartate, a caged compound for selective activation of glutamate transporters and N-methyl-D-aspartate receptors in brain tissue. Biochemistry 44:3316–3326.

Ito M, Kano M (1982) Long-lasting depression of parallel fiber-Purkinje cell transmission induced by conjunctive stimulation of parallel fibers and climbing fibers in the cerebellar cortex. Neurosci Lett 33:253–258.

Khaliq ZM, Raman IM (2005) Axonal propagation of simple and complex spikes in cerebellar Purkinje neurons. J Neurosci 25:454–463.

Kitazawa S, Kimura T, Yin PB (1998) Cerebellar complex spikes encode both destinations and errors in arm movement. Nature 392:494–497.

Lang EJ, Sugihara I, Welsh JP, Llinas R (1999) Patterns of spontaneous Purkinje cell complex spike activity in the awake rat. J Neurosci 19:2728–2739.

Liu G, Choi S, Tsien RW (1999) Variability of neurotransmitter concentration and nonsaturation of postsynaptic AMPA receptors at synapses in hippocampal cultures and slices. Neuron 22:395–409.

Llinas R, Baker R, Sotelo C (1974) Electrotonic coupling between neurons in cat inferior olive. J Neurophysiol 37:560–571.

Llinas R, Walton K, Hillman DE, Sotelo C (1975) Inferior olive: its role in motor learning. Science 190:1230–1231.

Maejima T, Hashimoto K, Yoshida T, Aiba A, Kano M (2001) Presynaptic inhibition caused by retrograde signal from metabotropic glutamate to cannabinoid receptors. Neuron 31:463–475.

Mathy A, Ho SS, Davie JT, Duguid IC, Clark BA, Häusser M (2009) Encoding of oscillations by axonal bursts in inferior olive neurons. Neuron 62:388–399.

Miledi R (1966) Strontium as a substitute for calcium in the process of transmitter release at the neuromuscular junction. Nature 212:1233–1234.

Moechars D, Weston MC, Leo S, Callaerts-Vegh Z, Goris I, Daneels G, Buist A, Cik M, van der Spek P, Kass S, Meert T, D'Hooge R, Rosenmund C, Hampson RM (2006) Vesicular glutamate transporter vGluT2 expression levels control quantal size and neuropathic pain. J Neurosci 26:12055–12066.

Monsivais P, Clark BA, Roth A, Hausser M (2005) Determinants of action potential propagation in cerebellar Purkinje cell axons. J Neurosci 25:464–472.

Nikkuni O, Takayasu Y, Iino M, Tanaka K, Ozawa S (2007) Facilitated activation of metabotropic glutamate receptors in cerebellar Purkinje cells in glutamate transporter EAAT4-deficient mice. Neurosci Res 59:296–303.

Nusser Z, Mulvihill E, Streit P, Somogyi P (1994) Subsynaptic segregation of metabotropic and ionotropic glutamate receptors as revealed by immunogold localization. Neuroscience 61:421–427.

O'Hearn E, Molliver ME (1997) The olivocerebellar projection mediates ibogaine-induced degeneration of Purkinje cells: a model of indirect, trans-synaptic excitotoxicity. J Neurosci 17:8828–8841.

Oliet SH, Malenka RC, Nicoll RA (1996) Bidirectional control of quantal size by synaptic activity in the hippocampus. Science 271:1294–1297.

Otis TS, Kavanaugh MP, Jahr CE (1997) Postsynaptic glutamate transport at the climbing fiber-Purkinje cell synapse. Science 277:1515–1518.

Ozden I, Sullivan MR, Lee HM, Wang SS (2009) Reliable coding emerges from coactivation of climbing fibers in microbands of cerebellar Purkinje neurons. J Neurosci 29:10463–10473.

Ozol K, Hayden JM, Oberdick J, Hawkes R (1999) Transverse zones in the vermis of the mouse cerebellum. J Comp Neurol 412:95–111.

Palkovits M, Mezey E, Hamori J, Szentagothai J (1977) Quantitative histological analysis of the cerebellar nuclei in the cat. I. Numerical data on cells and on synapses. Exp Brain Res 28:189–209.

Safo PK, Cravatt BF, Regehr WG (2006) Retrograde endocannabinoid signaling in the cerebellar cortex. Cerebellum 5:134–145.

Sasaki K, Bower JM, Llinas R (1989) Multiple Purkinje cell recording in rodent cerebellar cortex. Eur J Neurosci 1:572–586.

Shen Y, Linden DJ (2005) Long-term potentiation of neuronal glutamate transporters. Neuron 46:715–722.

Sugihara I, Wu HS, Shinoda Y (2001) The entire trajectories of single olivocerebellar axons in the cerebellar cortex and their contribution to cerebellar compartmentalization. J Neurosci 21:7715–7723.

Sugihara I, Marshall SP, Lang EJ (2007) Relationship of complex spike synchrony bands and climbing fiber projection determined by reference to aldolase C compartments in crus IIa of the rat cerebellar cortex. J Comp Neurol 501:13–29.

Sugihara I, Fujita H, Na J, Quy PN, Li BY, Ikeda D (2009) Projection of reconstructed single Purkinje cell axons in relation to the cortical and nuclear aldolase C compartments of the rat cerebellum. J Comp Neurol 512:282–304.

Szapiro G, Barbour B (2007) Multiple climbing fibers signal to molecular layer interneurons exclusively via glutamate spillover. Nat Neurosci 10:735–742.

Takayasu Y, Iino M, Kakegawa W, Maeno H, Watase K, Wada K, Yanagihara D, Miyazaki T, Komine O, Watanabe M, Tanaka K, Ozawa S (2005)

Differential roles of glial and neuronal glutamate transporters in Purkinje cell synapses. J Neurosci 25:8788–8793.

Telgkamp P, Raman IM (2002) Depression of inhibitory synaptic transmission between Purkinje cells and neurons of the cerebellar nuclei. J Neurosci 22:8447–8457.

Telgkamp P, Padgett DE, Ledoux VA, Woolley CS, Raman IM (2004) Maintenance of high-frequency transmission at Purkinje to cerebellar nuclear synapses by spillover from boutons with multiple release sites. Neuron 41:113–126.

Wadiche JI, Jahr CE (2001) Multivesicular release at climbing fiber-Purkinje cell synapses. Neuron 32:301–313.

Wadiche JI, Jahr CE (2005) Patterned expression of Purkinje cell glutamate transporters controls synaptic plasticity. Nat Neurosci 8:1329–1334.

Wadiche JI, Tzingounis AV, Jahr CE (2006) Intrinsic kinetics determine the time course of neuronal synaptic transporter currents. Proc Natl Acad Sci U S A 103:1083–1087.

Wang SSH, Denk W, Häusser M (2000) Coincidence detection in single dendritic spines mediated by calcium release. Nat Neurosci 3:1266–1273.

Wilson NR, Kang J, Hueske EV, Leung T, Varoqui H, Murnick JG, Erickson JD, Liu G (2005) Presynaptic regulation of quantal size by the vesicular glutamate transporter VGLUT1. J Neurosci 25:6221–6234.

Xu-Friedman MA, Regehr WG (2000) Probing fundamental aspects of synaptic transmission with strontium. J Neurosci 20:4414–4422.

Yang Y, Gozen O, Watkins A, Lorenzini I, Lepore A, Gao Y, Vidensky S, Brennan J, Poulsen D, Won Park J, Li Jeon N, Robinson MB, Rothstein JD (2009) Presynaptic regulation of astroglial excitatory neurotransmitter transporter GLT1. Neuron 61:880–894.